

Corrosion Rate and Remaining Lifetime Calculation of Shell and Tube Heat Exchanger XXX-E-XX Based on Eddy Current Test and Ultrasonic Thickness Measurement Inspection Methods in the Delayed Coker Unit Operation Area

¹Tony Suryo Utomo, ^{2*}Berkah Fajar TK, ³Hafiz Akbar Simanjorang

^{1,2,3}Mechanical Engineering Department, Diponegoro University, Jl. Prof Soedarto SH Tembalang, Semarang, Indonesia

Abstract - Shell and tube heat exchangers play a vital role in refinery operations by ensuring efficient heat transfer. However, corrosion significantly impacts their performance, reliability, and lifespan, leading to potential operational risks. This study assesses the corrosion rate and remaining lifetime of the shell and tube heat exchanger XXX-E-XX using Eddy Current Testing (ECT) for tube bundles and Ultrasonic Thickness (UT) measurement for the shell. The objective is to evaluate the extent of material degradation and predict the remaining service life based on API standards. Corrosion rates are determined by analyzing thickness reduction from historical inspection data, covering the period from 2016 to 2020. The results indicate that the corrosion rate of tube bundles ranges from 0.105 to 0.21 mm/y, while the shell exhibits a wider corrosion rate variation of 0.095 to 0.535 mm/y. The estimated remaining lifetime for tube bundles is between 5.28 and 14.56 years, whereas the shell components range from 1.89 to 43.09 years. To enhance operational reliability, periodic inspections, predictive maintenance strategies, and material improvements are recommended. These findings provide valuable insights into maintenance planning and longevity assessment of heat exchangers in refinery applications.

Keywords: Shell and Tube Heat Exchanger, Corrosion Rate, Remaining Lifetime, Eddy Current Testing, Ultrasonic Thickness Measurement, Material Degradation, Refinery Unit.

I. INTRODUCTION

The growing energy demand in Indonesia, particularly in the oil and gas sector, continues to rise alongside population growth, economic development, and industrial needs. Petroleum fuels remain the dominant energy source, requiring efficient and reliable refinery operations. Within refineries, heat exchangers play a vital role in heat transfer processes, especially in fractionation systems like the Delayed Coker Unit (DCU).

One critical component is the Shell and Tube Heat Exchanger, functioning as a debutanizer overhead condenser by transferring heat from hydrocarbon vapors to cooling seawater. Operating under high-temperature, multiphase flow conditions makes these exchangers prone to corrosion issues such as under-deposit corrosion (UDC), pitting, and stress corrosion cracking [1], [2], often leading to tube-to-tubesheet joint failures [3]. To maintain reliability, refineries implement routine inspections and scheduled Turn Around (TA) programs every four years, involving non-destructive testing (NDT) methods like Eddy Current Testing (ECT) and Ultrasonic Thickness Measurement (UTM) [4]. Recently, corrosion risk analysis using predictive simulations has enhanced maintenance strategies [5], as corrosion behavior tends to follow a bimodal progression influenced by operational conditions [6]. For Shell and Tube Heat Exchanger 140-E-20, ECT data from the 2020 TA and UTM data from the 2024 TA provide a basis to calculate corrosion rates and predict remaining lifetime. Hydrostatic testing is also conducted to verify system integrity. This study aims to analyze corrosion rates and remaining lifetime based on ECT and UTM data, providing technical recommendations for maintenance optimization and supporting reliability management in corrosion-prone units like the DCU [3], [7].

II. METHODOLOGY

2.1 Shell and Tube Heat Exchanger

Shell and tube heat exchangers are widely applied in oil and gas processing facilities for transferring thermal energy between two immiscible fluids separated by a solid metal wall, typically tube material [2]. They are favored in refineries and petrochemical plants for their high thermal efficiency, mechanical strength, and adaptability [2]. Structurally, this equipment consists of a cylindrical shell containing parallel tubes fixed by tube sheets, with one fluid flowing inside the tubes (tube-side) and another across the shell (shell-side). Baffles inside the shell enhance heat transfer by promoting cross-flow and turbulence [1]. In the Delayed Coker Unit (DCU), this exchanger serves as a debutanizer overhead

condenser, cooling hot hydrocarbon vapors through indirect contact with seawater, condensing them into liquid while separating non-condensable gases [3]. Its performance is affected by temperature, pressure, fouling, and flow distribution. Risks like ammonium chloride salt deposits can disrupt flow and trigger localized corrosion.

Shell and tube heat exchangers remain preferred due to their modular design, pressure resistance, and ease of maintenance during Turn Around (TA) programs [3]. To maintain integrity, periodic inspections target corrosion, wall thinning, leakage, and flow restrictions. Commonly used methods Ultrasonic Thickness Measurement (UTM) for shell-side evaluations [4].

2.2 Corrosion Identification

Heat exchangers include Eddy Current Testing (ECT) for tube-side and play a vital role in numerous industrial sectors, including oil and gas, chemical processing, pharmaceuticals, petroleum refining, and pulp and paper. These systems operate under varying environmental conditions, some of which are highly corrosive, posing a substantial challenge to equipment longevity and performance. In fact, a 2001 study estimated that corrosion in all forms imposed a direct economic burden of approximately \$276 billion per year in the United States, equivalent to about 3.1% of the country's GDP [7]. In the context of heat exchangers, corrosion not only reduces efficiency but also elevates maintenance frequency and costs. To address this, preventive measures such as optimized material selection, protective coatings, and the implementation of cathodic or anodic protection systems are commonly applied.

Uniform corrosion is one of the most common degradation mechanisms encountered in heat exchangers. It occurs when the material deteriorates evenly over the surface, leading to gradual wall thinning. This type of corrosion is relatively easy to detect visually, and though it may progress slowly, it can eventually result in structural failure due to reduced mechanical strength. The best approach to mitigate uniform corrosion is the use of corrosion-resistant materials that can form a stable passive film under operating conditions. Alternatively, conducting exposure or immersion tests prior to service can help quantify expected corrosion rates—typically expressed in millimeters per year (mm/year)—allowing engineers to design with sufficient corrosion allowance. Studies have shown that uniform corrosion is often more aggressive on the cooling water side than on the interior tube surfaces [8]. However, uniform corrosion is only part of the problem.

Localized corrosion, especially pitting, poses a greater threat to the structural integrity of heat exchangers. Pitting

corrosion arises when the protective oxide layer on a metal surface is locally breached, often due to mechanical damage or exposure to aggressive chemicals such as chlorides or acidic solutions. This can lead to deep, narrow cavities that are difficult to detect and monitor but can rapidly progress to through-wall perforation. Even corrosion-resistant materials like stainless steel and titanium are vulnerable to pitting when exposed to environments with high chloride content and low pH values [8]. The severity of pitting corrosion can be assessed using the Pitting Resistance Equivalent Number (PREN), a value derived from the alloy's composition—higher PREN values correlate with greater pitting resistance [10].

Another critical degradation mechanism is erosion corrosion, which combines mechanical wear from high-velocity fluids and chemical attack from the process medium. This typically occurs at fluid inlets, particularly in shell-and-tube heat exchangers, where it is known as inlet-tube corrosion. The presence of abrasive particles, such as sand, exacerbates the effect by stripping away protective films, leading to accelerated material loss. In real-world applications, such as geothermal power plants, erosion and pitting corrosion have been observed to cause significant damage. One notable case involved a shell-and-tube heat exchanger suffering severe pitting on its middle tubes due to acidic condensate containing CO₂ and H₂S, ultimately compromising the exchanger's operational integrity [9]. Overall, the selection of materials, understanding of fluid characteristics, and proper design adjustments are essential to ensure the durability and reliability of heat exchangers in corrosive service environments.

2.3 Inspection Methods

Eddy Current Testing (ECT) is a widely used non-destructive testing (NDT) method for detecting surface and subsurface defects in conductive materials, particularly in metal, nuclear, and aerospace industries. It operates by inducing circulating currents via an alternating magnetic field, where discontinuities alter the sensor's impedance [11]. ECT offers advantages such as high inspection speeds, non-contact testing, and the ability to measure conductivity and layer thickness [11]. Recent advancements include multi-frequency designs, Hall-effect sensors, magneto-resistive sensors, and Superconducting Quantum Interference Devices (SQUIDs) for improved defect detection sensitivity [12]. Techniques like pulsed eddy current and high-frequency differential ECT further enhance detection in applications like heat exchangers [13][14]. Optimized materials and advanced signal processing algorithms reduce signal noise and improve defect detection, especially for heat exchanger tubes under thermal cycling [15]. Innovations like Giant Magnetoresistance (GMR), Hall-

effect, and SQUID sensors have extended ECT’s capability for preventive maintenance and life prediction in critical equipment [16].

Ultrasonic Thickness Measurement (UTM) is a cornerstone technique in NDT for detecting wall thinning and corrosion in pipelines and heat exchanger components. Based on the time-of-flight (TOF) of ultrasonic pulses, its accuracy is influenced by temperature gradients. Two-sensor systems using compressive and shear wave modes, combined with non-iterative algorithms, enable real-time, high-accuracy thickness estimation under varying thermal conditions, achieving up to 98% reduction in measurement error compared to conventional single-mode systems [17]. Similar temperature compensation strategies integrating ultrasonic and thermal modeling have also been applied for structural monitoring [18][19]. Additionally, circumferential ultrasonic inspection using Continuous Wavelet Transform (CWT), Inverse CWT, and Deep Neural Networks (DNNs) has achieved 99.99% accuracy in identifying leaks in heat exchanger tubes and shells [20]. These advancements build on wavelet-based analysis frameworks that proved effective in ultrasonic guided wave filtering for complex structures and pipelines [21][22].

2.4 Required Thickness Determination

The required wall thickness is a critical parameter in pressure system design and must be determined before assessing corrosion or remaining life. For straight piping under internal pressure, ASME B31.3 provides the equation:

$$t = \frac{PD}{2(SEW + PY)}$$

Where P is the internal pressure, D is the outside diameter, S is the allowable stress, E is the longitudinal joint quality factor (typically 1.0 for seamless pipes), W is the weld joint factor (usually 1.0 for seamless pipes), and Y is a material-dependent coefficient.

For pressure vessel shells governed by circumferential stress—typically when the wall thickness is less than half the internal radius or the pressure does not exceed 0.385SE—the minimum required thickness is calculated as:

$$t_{min} = \frac{PR}{SE - 0.6P}$$

If longitudinal stress governs—generally when the pressure is less than 1.25SE or the wall thickness is still under half the radius—the formula becomes:

$$t_{min} = \frac{PR}{2SE - 0.4P}$$

In both equations, R is the internal radius, and values for S are obtained from ASME Section II, Part D, Table 1A, for instance, 108 MPa for SA-283 Grade C at 125 °C. The weld efficiency factor E, sourced from ASME Section VIII Table UW-12, is typically 0.85 or 1 depending on weld type and quality.

The calculation of the required thickness for the shell head refers to the ASME Section VIII, Division 1, UG-32, which covers formed heads and sections subjected to pressure on the concave side. In this case, the type used is an *ellipsoidal head* with a thickness-to-diameter ratio (*ts/L*) greater than or equal to 0.002.

$$t_{required} = \frac{PD}{2SE - 0.2P}$$

2.5 Corrosion Rate Calculation

Corrosion significantly affects the service life of heat exchanger components. To estimate remaining life, corrosion rate must be calculated using either the short-term (ST) or long-term (LT) method, as per API 570. The long-term corrosion rate reflects overall material loss since installation, while the short-term rate captures recent changes between two inspection dates. Both are calculated by dividing the thickness loss by the time interval.

$$\text{Corrosion Rate}_{(ST)} = \frac{t_{previous} - t_{actual}}{\text{time (years) between } t_{previous} \text{ and } t_{actual}}$$

Similarly, the long-term corrosion rate is:

$$\text{Corrosion Rate}_{(LT)} = \frac{t_{initial} - t_{actual}}{\text{time (years) between } t_{initial} \text{ and } t_{actual}}$$

2.6 Remaining Lifetime Calculation

According to API 510, the remaining life of a pressure vessel component is the estimated time it can continue operating before its wall thickness reaches the minimum allowable limit. This helps in scheduling inspections and maintenance. Remaining life is calculated by subtracting the required thickness from the current measured thickness, then dividing by the corrosion rate:

$$\text{Remaining Lifetime}_{(RL)} = \frac{t_{actual} - t_{required}}{\text{corrosion Rate (mmpy)}}$$

$t_{required}$ is the required minimum thickness of the component (in mm or inches), determined based on design calculations and including corrosion and manufacturing tolerances. t_{actual} is the most recent measured thickness at the same location.

III. RESULTS AND DISCUSSIONS

3.1 Heat Exchanger Specification and Condition

The technical specifications of the Shell and Tube Heat Exchanger XXX-E-XX used in this study are presented in Table 1 below.

Table 1: Technical Specifications of Shell and Tube Heat Exchanger XXX-E-XX

Name of Equipment	: Debutanizer Overhead Condenser		
Vessel Position	: Horizontal		
Inspection Date	: 21/12/24		
Last Inspection Date	: 09/12/20		
Design & Operation Data			
Data	Shell	Head	Channel
Design Pressure (kg/cm ² .g)	18.3	18.3	10.8
Design Temperature	120° C	120° C	120° C
Op. Pressure (kg/cm ² .g)	16.10	16.10	3.20
Op. Temperature	72° C	72° C	38° C
Nozzles and Manways			
Mark	Qty	Size	Fluid
N1	1	10"	Sea Water Inlet
N2	1	10"	Sea Water Outlet
N3	1	8"	Hydrocarbon Inlet
N4	1	8"	Hydrocarbon Outlet

3.2 Eddy Current Test Inspection for Tube Sheet Result

Non-destructive inspection was conducted on the tube bundles of Heat Exchanger 140-E-20 using the Eddy Current Test (ECT) method to assess the integrity and detect wall thinning defects. In accordance with the established defect classification standards, the degree of wall loss was categorized into four classes based on the percentage of material loss, as presented in Table 2 below:

Table 2: Category of Defective Tubes (% Wall Loss)

Class	Range of Defect	Colour
1	0 – 20 %	
2	21% – 40%	
3	41% – 60%	

4	69% – 100%	
---	------------	---

To facilitate the identification of defective tubes, a systematic numbering method was applied on the tubesheet. The horizontal axis (X-axis) was designated for column numbering (1, 2, 3,...), while the vertical axis (Y-axis) was used for row numbering (1, 2, 3, ...). This approach ensured precise localization and traceability of each tube's inspection result, as illustrated in Figure 1 below.

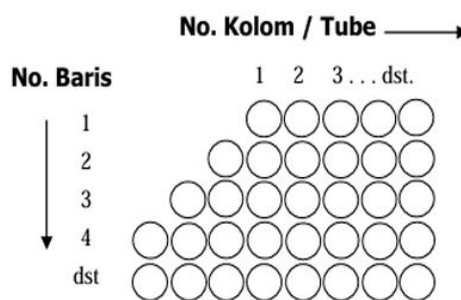


Figure 1: Systematic Numbering Method for Tubesheet Inspection

The inspection covered a total of 390 tubes out of 760, representing approximately 51.3% of the total tube population. The detailed ECT inspection results are presented in Table 3 below.

Table 3: Eddy Current Test Inspection Results of Tube Bundles

Tube Specification and Inspection Data				
Material	OD (mm)	Thick. (mm)	Total Tube	Tube Inspected
SB111C715	25.4	2.11	760	390
Wall Loss Classification (%)				
0 - 21	21-40	41-60	>60	Stuck
361	19	-	-	10

Figure 2 visualizes each tube's condition and categorizes wall loss percentages accordingly.

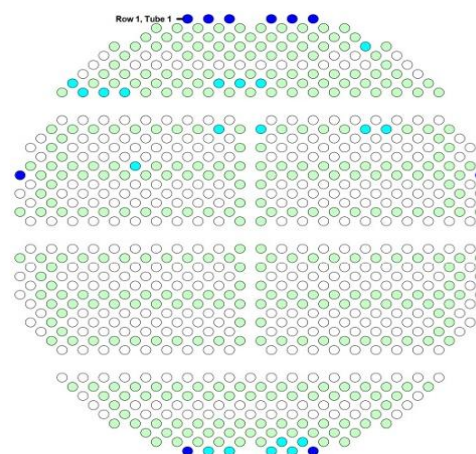


Figure 2: Mapping of Tube Wall Thickness Classification

3.3 Ultrasonic Thickness Inspection for Shell Result

The inspection mapping for Shell and Tube Heat Exchanger 140-E-20 included multiple measurement points at nozzle locations (N1-N4) and shell sections (A-F) as illustrated in Figure 3 below.

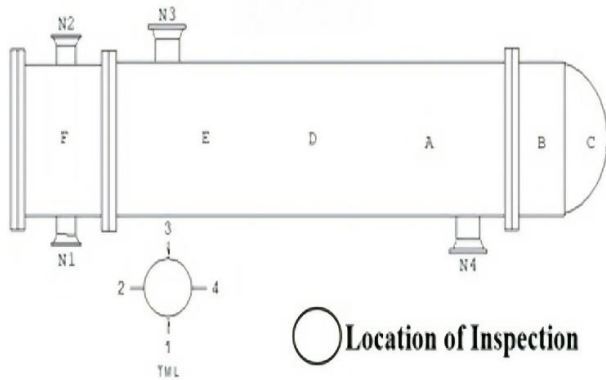


Figure 3: UT Measurement inspection mapping for Shell

Based on the ultrasonic thickness inspection conducted in 2024 compared to baseline measurements from 2020, the detailed measurement results are presented in Table 4 below:

Table 4: Results of Ultrasonic Thickness Measurement on Shell

Location	Actual Thickness At Position (mm)					2024 Thickness
	2020 Thickness	1	2	3	4	
N1	12.25	11.17	11.13	11.09	10.67	10.67
N2	12.31	11.46	11.06	12.20	11.80	11.06
N3	12.23	11.12	11.34	11.24	11.72	11.12
N4	12.25	11.38	12.02	11.98	11.93	11.38
A	16.60	16.21	16.15	16.32	16.24	16.15
B	17.68	16.23	17.32	16.76	17.27	16.23
C	16.88	16.45	16.45	16.32	16.19	16.19
D	17.22	16.63	16.41	16.40	16.16	16.16
E	16.17	15.86	15.79	16.04	15.82	15.79
F	9.65	9.52	9.37	9.31	9.48	9.31

Ultrasonic thickness measurements show varying wall thinning in the heat exchanger shell. Nozzle areas (N1–N4) range from 10.67 mm to 12.31 mm, while shell sections (A–F) vary between 9.31 mm and 17.68 mm. The thinnest point is at location F (9.31 mm), marking it as a critical area. A comparison of 2020 baseline data with 2024 results reveals consistent material loss across all locations. Notably, N1 and F show the highest reductions, with thickness decreasing by 12.9% and 12.8%, respectively. These trends are illustrated in Figure 4, which highlights the most affected zones.

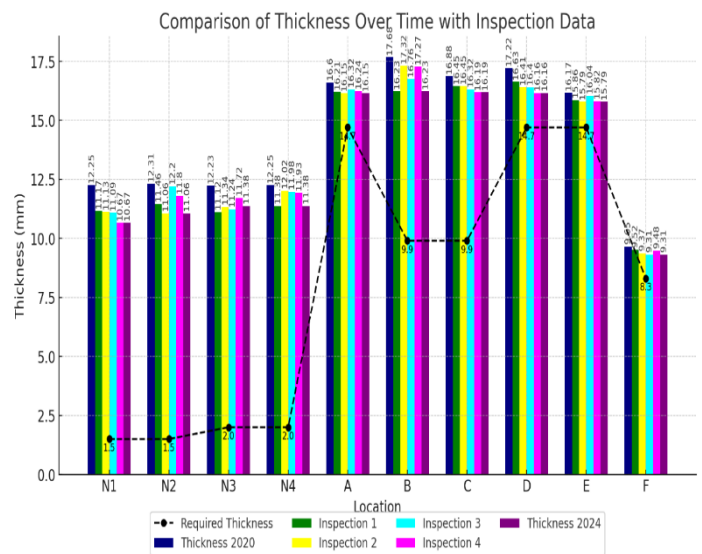


Figure 4: Comparison of Measured Wall Thickness on the Shell of Heat Exchanger XXX-E-XX Graphic

The graph includes a dashed line indicating the required minimum thickness, allowing quick identification of critical areas. Although all locations show material loss, current thicknesses remain above the minimum, confirming safe operation. Sections A–E retain higher values (15.79–16.23 mm), while section F shows notably lower readings, indicating possible localized degradation that warrants closer monitoring in future inspections.

3.4 Required Thickness Calculation

These calculations establish reference values for assessing equipment integrity based on design criteria and safety factors. Required thicknesses were derived using ASME code equations tailored to each component’s geometry and function, considering pressure, allowable stress, joint efficiency, and corrosion allowance. ASME B31.3 was used for tubes, while shells and heads were evaluated per ASME Section VIII, Division 1—UG-27 for shells and UG-32 for ellipsoidal heads ($ts/L \geq 0.002$). Material properties were sourced from ASME Section II based on each component’s grade.

Tube Bundles: Based on The ASME Section II, Part D, SB-111 C71500 tubes with design temperature of 120°C and allowable stress of 82.7MPa require a minimum thickness of 0.161 mm to withstand operational pressures safely.

$$t_{required} = \frac{PD}{2(SEW + PY)}$$

$$t_{required} = \frac{(1,059)(25,4)}{2((82,7)(1)(1) + (1,059)(0,4))}$$

$$t_{required} = 0,161 \text{ mm}$$

Shell: The calculation employed the formula specified in ASME Section VIII, Division 1, UG-27 with shell material is SA-285 Gr.C. To determining the required thickness of shells under internal pressure circumferential stress (longitudinal joints) type.

$$t_{required} = \frac{PR}{SE-0.6P} + CA$$

$$t_{required} = \frac{(1,79)(584)}{(108)(0,85)-0,6(1,79)} + 3,2$$

$$t_{required} = 11,5 + 3,2$$

$$t_{required} = 14,7 \text{ mm}$$

Channel: The equation applied in this analysis follows ASME Section VIII, Division 1, UG-27 for calculating the required shell thickness under internal pressure, addressing circumferential stress (longitudinal joints), with SB-169 Cl.61400 material.

$$t_{required} = \frac{PR}{SE-0.6P} + CA$$

$$t_{required} = \frac{(1,059)(584)}{(142)(0,85)-0,6(1,059)}$$

$$t_{required} = 5,1 + 3,2$$

$$t_{required} = 8,3 \text{ mm}$$

Nozzle Pipe Shell Side: According to ASME B31.3, the material SA-106 Gr. B, classified under UNS K03006 and designed for a temperature of 120°C, has an allowable stress of 118 MPa.

$$t_{required} = \frac{PD}{2(SEW+PY)}$$

$$t_{required} = \frac{(1,79)(219)}{2((118)(1)(1)+(1,79)(0,4))}$$

$$t_{required} = 2,0 \text{ mm}$$

Nozzle Pipe Channel Side: For the material SA-106 Gr. A, corresponding to UNS K02501 at a design temperature of 120°C, the allowable stress is specified as 94.5 MPa.

$$t_{required} = \frac{PD}{2(SEW+PY)}$$

$$t_{required} = \frac{(1,059)(273)}{2((94,5)(1)(1)+(1,059)(0,4))}$$

$$t_{required} = 1,5 \text{ mm}$$

Shell Head: The equation used in this analysis refers to ASME Section VIII, Division 1, UG-32 with shell head material is SA-285 Gr.C. To determining the thickness of formed heads subjected to internal pressure on the concave side, applicable to ellipsoidal heads with a ts/L ratio greater than or equal to 0.002.

$$t_{required} = \frac{PD}{2SE-0.2P} + CA$$

$$t_{required} = \frac{(1,059)(1168)}{2(108)(0,85)-(0,2)(1,059)} + 3,2$$

$$t_{required} = 9,9 \text{ mm}$$

3.5 Corrosion Rate Calculation

The detailed calculation results of the short-term corrosion rate for the tube bundles are presented in Table 5 below:

Table 5: Short-term corrosion rate for the tube bundles

Wall Loss (%)	$T_{Previous}$ (2016)	T_{actual} (2020)	Corrosion rate	
			mm/year	Inch/year
0-20%	2.11 mm	2.11 mm	0	0
		1.69 mm	0.105	0.00413
21-40%	2.11 mm	1.67 mm	0.11	0.00433
		1.27 mm	0.21	0.00827

The results of the long-term corrosion rate calculation for the tube bundles are summarized in Table 6 below:

Table 6: Long-Term Corrosion Rate for the Tube Bundles

Wall Loss (%)	$T_{Previous}$ (1981)	T_{actual} (2020)	Corrosion rate	
			mm/year	Inch/year
0-20%	2.11 mm	2.11 mm	0	0
		1.69 mm	0.0108	0.000425
21-40%	2.11 mm	1.67 mm	0.0113	0.000445
		1.27 mm	0.0215	0.000846

The corrosion rate values for the shell side based on the short-term calculation are shown in Table 7 below:

Table 7: The Short-Term Corrosion Rate for the Shell Side

Location	$T_{Previous}$ (2020)	T_{actual} (2024)	Corrosion rate	
			mm/year	Inch/year
N1	12.25	10.67	0.395	0.0156
N2	12.31	11.06	0.3125	0.0123
N3	12.23	11.12	0.2775	0.0109
N4	12.25	11.38	0.2175	0.0086
A	16.60	16.15	0.1125	0.0044
B	17.68	16.23	0.3625	0.0143
C	16.88	16.19	0.1725	0.0068
D	17.22	16.16	0.265	0.0104

E	16.17	15.79	0.095	0.0037
F	11.45	9.31	0.535	0.0211

The long-term corrosion rate data for the shell side is displayed in Table 8 below:

Table 8: Long-Term Corrosion Rate for the Shell Side

Location	$T_{Previous}$ (1981)	T_{actual} (2024)	Corrosion rate	
			mm/year	Inch/year
N1	12.70	10.67	0.0472	0.00186
N2	12.70	11.06	0.0381	0.00150
N3	12.70	11.12	0.0367	0.00144
N4	12.70	11.38	0.0307	0.00121
A	17.00	16.15	0.0198	0.00078
B	18.00	16.23	0.0412	0.00162
C	18.00	16.19	0.0421	0.00166
D	17.00	16.16	0.0195	0.00077
E	17.00	15.79	0.0281	0.00110
F	10.00	9.31	0.0160	0.00063

3.6 Remaining Lifetime Calculation

The calculation of the remaining life of the Tube Bundles section of the shell and tube heat exchanger equipment in the DCU area can be seen in table 9 below:

Table 9: Remaining lifetime of the Tube Bundles

Wall Loss(%)	$T_{required}$ (mm)	T_{actual} (2020) (mm)	ST Corrosion Rate (mm/year)	Remaining Lifetime (years)
0-20%	0,161	1.69	0.105	14,56
	0,161	1.67	0.11	13,72
21-40%	0,161	1.27	0.21	5,28

The calculation of the remaining life of the shell side of the shell and tube heat exchanger equipment in the DCU area can be seen in table 10 below:

Table 10: Remaining lifetime of the Shell

Sides	Location	$T_{required}$ (mm)	T_{actual} (2024)	Corrosion Rate	Remaining Lifetime (years)
Nozzle	N1	1,5	10.67	0.395	23.19
Nozzle	N2	1,5	11.06	0.3125	30.59
Nozzle	N3	2,0	11.12	0.2775	32.85
Nozzle	N4	2,0	11.38	0.2175	43.09
Shell	A	14.7	16.15	0.1125	12.44
Head	B	9,9	16.23	0.3625	17.47
Head	C	9,9	16.19	0.1725	36.47
Shell	D	14.7	16.16	0.265	5.51
Shell	E	14.7	15.79	0.095	11.37
Channel	F	8.3	9.31	0.535	1.89

IV. CONCLUSION

This study successfully evaluated the corrosion rate and remaining lifetime of the Shell and Tube Heat Exchanger XXX-E-XX operating in the Delayed Coker Unit area by employing Eddy Current Testing (ECT) and Ultrasonic Thickness Measurement (UTM) inspection methods. From the ECT results, out of 760 tubes, 361 tubes were found within safe thinning limits (0–20%), while 19 tubes experienced moderate thinning (21–40%), and no tubes exceeded 40% wall loss, confirming acceptable operational integrity for the tube bundle section. The UTM inspection revealed localized wall thinning on the shell side, with the lowest thickness recorded at 9.31 mm in Section F, although still above the required minimum threshold of 8.3 mm for that region. The short-term corrosion rates ranged from 0.095 to 0.535 mm/y for the shell and 0.105 to 0.21 mm/y for the tube bundles, which provided an accurate basis for remaining life estimations. The remaining lifetime of tube bundles was predicted between 5.28 and 14.56 years, while the shell side varied from 1.89 to 43.09 years, depending on specific component locations. These findings directly address the research objective by quantifying material degradation trends and predicting service life based on standardized API procedures. Furthermore, the study highlights that Section F on the shell side and several moderate-loss tubes in the bundle require increased inspection frequency and potential preventive action during the next Turn Around (TA). To enhance operational reliability, future research should focus on implementing Pulsed Eddy Current (PEC) for improved detection of subsurface flaws and integrating advanced data processing algorithms such as deep neural networks (DNN) and machine learning-based defect classification as demonstrated by Malikov et al. and Alvarenga et al. Additionally, real-time corrosion monitoring using multi-sensor ECT systems and temperature-compensated UTM strategies like those proposed by Palanisamy et al. are recommended for continuous asset integrity management in refinery environments.

REFERENCES

- [1] X. Liu, H. Zhu, C. Yu, H. Jin, C. Wang, and G. Ou, "Analysis on the corrosion failure of U-tube heat exchanger in hydrogenation unit," *Eng. Fail. Anal.*, vol. 125, p. 105448, 2021, doi: 10.1016/j.engfailanal.2021.105448.
- [2] W. Faes, S. Lecompte, Z. Y. Ahmed, et al., "Corrosion and corrosion prevention in heat exchangers," *Corros. Rev.*, 2019, doi: 10.1515/correv-2018-0054.
- [3] Z. Jin and X. Li, "Failure analysis and preventative measures on cracking of tube-to-tubesheet joints of the large-scale heat exchanger," *Eng. Fail. Anal.*, vol. 163,

- p. 108630, 2024, doi: 10.1016/j.engfailanal.2024.108630.
- [4] T. Baba, S. Harada, H. Asano, et al., "Nondestructive inspection for boiling flow in plate heat exchanger by neutron radiography," *Nucl. Instrum. Methods Phys. Res. A*, vol. 605, no. 1–2, pp. 142–145, 2009, doi: 10.1016/j.nima.2009.01.140.
- [5] H.-Z. Jin, Y. Gu, and G.-F. Ou, "Corrosion risk analysis of tube-and-shell heat exchangers and design of outlet temperature control system," *Pet. Sci.*, vol. 18, pp. 1219–1229, 2021, doi: 10.1016/j.petsci.2021.07.002.
- [6] R. E. Melchers, R. Jeffrey, I. A. Chaves, and R. B. Petersen, "Predicting corrosion for life estimation of ocean and coastal steel infrastructure," *Mater. Corros.*, vol. 75, no. 2, pp. 163–175, 2024, doi: 10.1002/maco.202314201.
- [7] G. H. Koch, M. P. H. Brongers, N. G. Thompson, Y. P. Virmani, and J. H. Payer, Corrosion Costs and Preventive Strategies in the United States. *U.S. Federal Highway Administration*, 2002, doi: 10.1061/9780784413586.ch01.
- [8] R. W. Revie and H. H. Uhlig, Corrosion and Corrosion Control: An Introduction to Corrosion Science and Engineering, 4th ed. Hoboken, NJ: John Wiley & Sons, 2008, doi: 10.1002/9780470277270.
- [9] Thulukkanam, Kuppan. Heat Exchanger Design Handbook. 1st ed. Boca Raton: CRC Press, 2000. <https://doi.org/10.1201/9781420026870>.
- [10] Roberge, Pierre R. Handbook of Corrosion Engineering. Vol. 1128. New York: McGraw-Hill, 2000.
- [11] García-Martín, Javier, Jaime Gómez-Gil, and Ernesto Vázquez-Sánchez. "Non-Destructive Techniques Based on Eddy Current Testing." *Sensors* 11, no. 3 (2011): 2525–2565. <https://doi.org/10.3390/s110302525>.
- [12] Sophian, Ali, Guiyun Tian, and Mengbao Fan. "Pulsed Eddy Current Non-Destructive Testing and Evaluation: A Review." *Chinese Journal of Mechanical Engineering* 30, no. 3 (2017): 500–514. <https://doi.org/10.1007/s10033-017-0122-4>.
- [13] AbdAlla, A.N., Faraj, M.A., Samsuri, F., Rifai, D., Ali, K., and Al-Douri, Y. "Challenges in Improving the Performance of Eddy Current Testing: Review." *Measurement and Control* 52, no. 4–5 (2019): 46–64. <https://doi.org/10.1177/0020294019835232>.
- [14] Alvarenga, T.A., Carvalho, A.L., Honorio, L.M., Cerqueira, A.S., Filho, L.M.A., and Nobrega, R.A. "Detection and Classification System for Rail Surface Defects Based on Eddy Current." *Sensors* 21, no. 21 (2021): 7937. <https://doi.org/10.3390/s21217937>.
- [15] A.D. Goodall, L. Chechik, R. L. Mitchell, G. W. Jewell, and I. Todd, "Cracking of soft magnetic FeSi to reduce eddy current losses in stator cores," *Additive Manufacturing*, vol. 70, 2023, Art. no. 103555. doi: <https://doi.org/10.1016/j.addma.2023.103555>
- [16] Machado, Miguel A. "Eddy Currents Probe Design for NDT Applications: A Review." *Sensors* 24, no. 17 (2024): 5819. <https://doi.org/10.3390/s24175819>.
- [17] Palanisamy, R.P., Pyun, D.-K., and Findikoglu, A.T. "Accurate Ultrasonic Thickness Measurement for Arbitrary Time-Variant Thermal Profile." *Sensors* 24, no. 16 (2024): 5304. <https://doi.org/10.3390/s24165304>.
- [18] Rommetveit, T., Johansen, T.F., and Johnsen, R. "A Combined Approach for High-Resolution Corrosion Monitoring and Temperature Compensation Using Ultrasound." *IEEE Transactions on Instrumentation and Measurement* 59, no. 10 (2010): 2843–2853. <https://doi.org/10.1109/TIM.2010.2046598>.
- [19] Zhang, Y., Cegla, F., and Corcoran, J. "Ultrasonic Monitoring of Pipe Wall Interior Surface Temperature." *Structural Health Monitoring* 20, no. 7 (2021): 2476–2492. <https://doi.org/10.1177/1475921720957592>.
- [20] Malikov, A.K., Cho, Y., Kim, Y.H., Kim, J., and Kim, H.K. "A Novel Ultrasonic Inspection Method of the Heat Exchangers Based on Circumferential Waves and Deep Neural Networks." *Science Progress* 106, no. 1 (2023): 1–26. <https://doi.org/10.1177/00368504221146081>.
- [21] Liu, T., Li, J., Cai, X., et al. "A Time-Frequency Analysis Algorithm for Ultrasonic Waves Generating from a Debonding Defect Using Empirical Wavelet Transform." *Applied Acoustics* 131 (2018): 16–27. <https://doi.org/10.1016/j.apacoust.2017.10.002>.
- [22] Siqueira, M.H.S., Gatts, C.E.N., Da Silva, R.R., et al. "The Use of Ultrasonic Guided Waves and Wavelet Analysis in Pipe Inspection." *Ultrasonics* 41, no. 10 (2004): 785–797. <https://doi.org/10.1016/j.ultras.2004.02.013>.

Citation of this Article:

Tony Suryo Utomo, Berkah Fajar TK, & Hafiz Akbar Simanjanorang. (2025). Corrosion Rate and Remaining Lifetime Calculation of Shell and Tube Heat Exchanger XXX-E-XX Based on Eddy Current Test and Ultrasonic Thickness Measurement Inspection Methods in the Delayed Coker Unit Operation Area. *International Research Journal of Innovations in Engineering and Technology - IRJIET*, 9(5), 254-262. Article DOI <https://doi.org/10.47001/IRJIET/2025.905034>
